Author version

Final publication: Dalski A, Kovács G, Ambrus GG. 2021. Evidence for a General Neural Signature of Face Familiarity. *Cerebral Cortex*, bhab366, https://doi.org/10.1093/cercor/bhab366

Evidence for a General Neural Signature of Face Familiarity

Alexia DALSKI[1,2,3], **Gyula KOVÁCS**[1] and **Géza Gergely AMBRUS**[1]

[1]Institute of Psychology, Friedrich Schiller University Jena, D-07743 Jena, Germany

[2]Department of Psychology, Philipps-Universität Marburg, D-35039 Marburg, Germany

[3]Center for Mind, Brain and Behavior – CMBB, Philipps-Universität Marburg and Justus-Liebig-Universität Giessen, D-35039 Marburg, Germany

Corresponding author: Géza Gergely Ambrus, Institute of Psychology, Friedrich Schiller University Jena, Leutragraben 1, D-07743 Jena, Germany. Email: g.ambrus@gmail.com,
ORCID iD: 0000-0002-8400-8178

Abstract

We explored the neural signatures of face familiarity using cross-participant and cross-experiment decoding of event-related potentials, evoked by unknown and experimentally familiarized faces from a set of experiments with different participants, stimuli, and familiarization-types. Human participants of both sexes were either familiarized perceptually, via media exposure, or by personal interaction. We observed significant cross-experiment familiarity decoding involving all three experiments, predominantly over posterior and central regions of the right hemisphere in the 270–630 ms time window. This shared face familiarity effect was most prominent across the Media and the Personal, as well as between the Perceptual and Personal experiments. Cross-experiment decodability makes this signal a strong candidate for a general neural indicator of face familiarity, independent of familiarization methods, participants, and stimuli. Furthermore, the sustained pattern of temporal generalization suggests that it reflects a single automatic processing cascade that is maintained over time.

Keywords: cross-experiment multivariate pattern analysis, EEG, face processing, familiarity, MVPA, person recognition

Introduction

The successful recognition of a face requires the interplay between multiple cognitive systems via connections across several parts of the brain. A number of regions have been shown to highly favor face stimuli, while others are known to carry out more general-purpose processing (Duchaine and Yovel 2015). The joint, synchronized functioning of this network enables the integration of perceptual, episodic and recognition memory, semantic, contextual and affective information that underlies everyday interactions with others (Kovács 2020).

We know relatively little about how this system accommodates the addition of a new face-identity to the existing repertoire of previously learned faces. To study the process of becoming familiar with someone, it is a good starting point to ask if a neural signature exists that reliably f lags unknown

and/or known faces, irrespective of the mode of acquisition or depth of encoding. Furthermore, should such signals exist, are they shared across individuals, implying more of an automatic processing cascade, or do they rather arise as a combination of stimulus properties and idiosyncratic activation patterns, shaped by the person's prior experience and functional-anatomical mappings (Wilmer et al. 2010; Verhallen et al. 2016; Sanchez et al. 2021)?

While the answer is most certainly a combination of both, compelling evidence exists for the markedly differential processing of familiar and unfamiliar faces (for a review see e.g., Johnston and Edmonds 2009). For example, in the macaque brain, images of personally familiar conspecifics engage the face processing network more than unfamiliar ones, and recruit additional areas in the perirhinal cortex and temporal pole that rapidly activate when familiar faces became recognizable (Landi and Freiwald 2017). Strong evidence from patients with acquired prosopagnosia (a brain-lesion-caused inability to recognize or experience a conscious feeling of familiarity with the faces of people previously encountered) provide clues that face familiarity can be inferred from physiological signals even without conscious recognition. Tranel and Damasio (1985) describe two female patients with bilateral occipito-temporal lesions who have shown elevated electrodermal responses for person ally familiar faces even in the absence of recall. Conversely, in Capgras syndrome person identification remains preserved but the associated feeling of familiarity appears to be lost and, in contrast to prosopagnosia, skin conductance responses do not differentiate between familiar and unfamiliar faces (Ellis and Lewis 2001). In healthy volunteers, eye movement patterns reveal distinct markers of familiar face recognition (Rosenzweig and Bonneh 2019) that may even defy active countermeasures at concealment (Millen and Hancock 2019).

In a recent study, Yan et al. (2017) demonstrated that while the processing of unfamiliar faces is not entirely automatic, familiarity with a face does increase the automaticity for certain facial characteristics. In a matching task, participants were instructed to report whether certain properties (sex, identity, ethnicity, and expression) were the same or different for two briefly presented faces. Automaticity was tested by comparing performance between cases when the instruction was given at the beginning of the trial to when it was given at the end of the trial. While performance for ethnicity (white/black) and expressed emotion (neutral/happy) benefited from cues at the beginning of the trial for both familiar and unfamiliar faces, no differences were found for judgments of sex and identity from familiar faces (celebrities), indicating a strong automatic processing of these dimensions. In agreement with this finding, Dobs et al. (2019) observed that familiarity enhanced the decodability of sex and identity (but not age) information at early stages of visual processing, suggesting that this

familiarity enhancement effect is due to these processes being tuned to familiar face features. In a change-detection task, which did not require explicit image recognition, Buttle and Raymond (2003) presented briefly and successively pairs of faces (either famous or recently learned), changing one of the two faces between the presentations, and found that the change-detection performance was significantly better for famous when compared to unknown faces. Also, the authors found a clear left visual filed bias, consistent with the view that the right hemisphere is involved in a more global mode of face processing, whereas the left hemisphere attends to local information, suggesting that extensive experience with a face gives rise to a more configural as opposed to a featural mode of face processing. Measuring visual search performance with familiar (male Hollywood actors) and unfamiliar faces in paradigm, Persike et al. (2013) found that face familiarity also strongly enhances performance, both in terms of accuracy and reaction time. While for target absent trials only a small familiarity advantage was shown, for target-present trials the effect was pronounced. Moreover, participants needed more than twice the time to process one item of unfamiliar, compared to familiar faces. The authors concluded that familiarity enhances difference detection among faces via efficient global mechanisms, connected to long term memory representations.

As we have seen, compelling evidence exists for differential processing of familiar and unfamiliar faces, implying the existence of automatic processes that provide prioritized access to certain stimulus characteristics when compared to faces of unknown individuals. The next logical question is, does this processing happen in a cascade-like manner with each step prewired, in temporal order, linked to the activity of distinct areas of the brain? Magnetoencephalography (MEG) and electroencephalography (EEG) provide the adequate temporal resolution to answer these questions and uncover the temporal dynamics underlying the emergence of face familiarity.

Previous research had identified several electrophysiological components that appear to be indicative of the processing of face stimuli. Very early processing differences for familiar and unfamiliar faces have been found across various studies by Caharel and colleagues (Caharel et al. 2009, 2013; Ramon et al. 2011).

The earliest of these components, the P1 (around 70–110 ms, with typically occipital peak) and the N170 (around 160–200 ms, with a lateral-parieto-occipital peak) most probably reflect early perceptual stages as they appear to be strongly modulated by the physical properties of the stimuli (Ambrus, Kaiser, et al. 2019).

It is important to note that familiarity information may indeed already be present in this time-window, but due to methodological constrains, its signals do not reach the surface sensors, or they are drowned out by the strong response produced by the rapid processing of physical features immediately after stimulus onset. A strong indication of this is the fact that in some cases even these early waves have been reported to be influenced by familiarity (Debruille et al. 1998; Caharel et al. 2002; Barragan-Jason et al. 2015), depending on the task, stimulus set, or prior expectations (Johnston et al. 2016). Furthermore, behavioral studies with high temporal precision, such as speeded go/no-go response tasks, eye movements or saccadic reaction times also support the idea that familiarity information may indeed already be present a very early stage (van Belle et al. 2010; Ramon et al. 2011, 2019).

The first ERP component that is behaviorally connected to recognition seems to be the N250, a parieto-occipital negative def lection between ca. 230 and 350 ms. Huang et al. (2017) found a positive correlation between the N250 amplitude and reaction time in a famous/non-famous decision task, suggesting that it is the earliest electrophysiological indicator of familiar face recognition in long-term memory.

More recently, several studies reported finding a late electrophysiological correlate of familiarity in the 400–600 ms time range. Using MEG, Dobs et al. (2019) observed a generic familiarity-related component ca. 400–600 ms after stimulus onset. Karimi-Rouzbahani et al. (2020) found a similar familiarity-related effect in EEG starting around 200 ms and peaking after approximately 400 ms. Wiese et al. (2019) observed an ERP component (dubbed as sustained familiarity effect, SFE) starting 200 ms after stimulus onset with a maximum between 400 and 600 ms and being the most prominent over bilateral posterior regions for highly familiar versus unfamiliar faces. Finally, in our previous multivariate pattern analysis (MVPA) studies we found image-independent identity effects (Ambrus, Kaiser, et al. 2019) and familiarity effects (Ambrus et al. 2021) falling within the same temporal range.

This study sets out to further investigate the spatio-temporal dynamics of the neural correlates of face familiarity by asking if a general, automatic signal of face familiarity processing exists, independent of participants, the properties of the stimuli, and the type of familiarization. As an extreme, and somewhat simplified example, we should find these hypothesized neural signatures in Alice when she meets her grandmother **for** a coffee, and in Bob, when he sees a known celebrity on the cover of a magazine while causally browsing at a newsstand. To investigate if representations are shared across participants and experimental conditions, a multivariate approach is necessary. Conventional univariate ERP analysis techniques contrast evoked response amplitudes between conditions at single or averaged channels, can tell us if the brain processes information differentially at a given time window. Instead of focusing on aggregated responses restricted in space and time, MVPA parses distributed patterns of activity at the trial level. It uses machine learning whereby the evoked responses from trials are iteratively split into training and test sets, and a classifier attempts to classify test trials based on the information it extracted from the training data. The classifier accuracy is therefore indicative of the presence of information in the pattern of evoked responses about the categories of interest (Grootswagers et al. 2017). A further advantage of MVPA over conventional ERP analysis is the flexibility that the train and test data need not necessarily come from the same time point, region of interest, experimental condition, participant, or, as we will see, from the same experiment.

To investigate the shared neural signatures of face familiarity we analyzed ERP data from three different experiments that utilized different (Perceptual, Media, and Personal) familiarization methods. Utilizing a thus far less explored multivariate cross-classification analysis (MVCC, Kaplan et al. 2015), we iteratively trained and tested on data from each experiment. This cross-experiment analysis combines elements of cross-modal, cross-participant, and leave-one-participant-out approaches. It is cross-modal in the sense that the mode of familiarization differed across the experiments and cross-participant as the experiments were conducted on different sets of volunteers. It is also similar to a leave-one-participant-out strategy as training is performed on concatenated data from multiple participants and tested on one participant at a time. We believe that this procedure is well-suited to find general neural patterns that are indicative of shared information processing.

Methods

Datasets

Three experiments, described in detail in a previous report from our laboratory, form the basis of the present study (Ambrus et al. 2021). These experiments investigated the EEG correlates of face familiarity in different familiarization conditions, using perceptual, media, and personal familiarization methods. The experiment was conducted in accordance with the guidelines of the Declaration of Helsinki, and with the approval of the ethics committee of the University of Jena. Written informed consent was acquired from all participants.

For details on stimulus presentation, data acquisition and preprocessing, see Ambrus et al. (2021). Briefly, stimuli were ambient face images, in color, depicting originally unfamiliar identities. The images were cropped to center on the inner features of the face, eye aligned, and were presented centrally on a uniform gray background in a pseudorandom order. In all cases, the stimulus presentation time was 600 ms. Spatial and temporal jitter was applied when presenting the stimuli. Participants were given a simple target detection task to ensure maintained attention throughout the sessions. No participant took part in more than one experiment. For the purposes of the current analysis, data for each participant were labeled on the familiarized/unknown dimension.

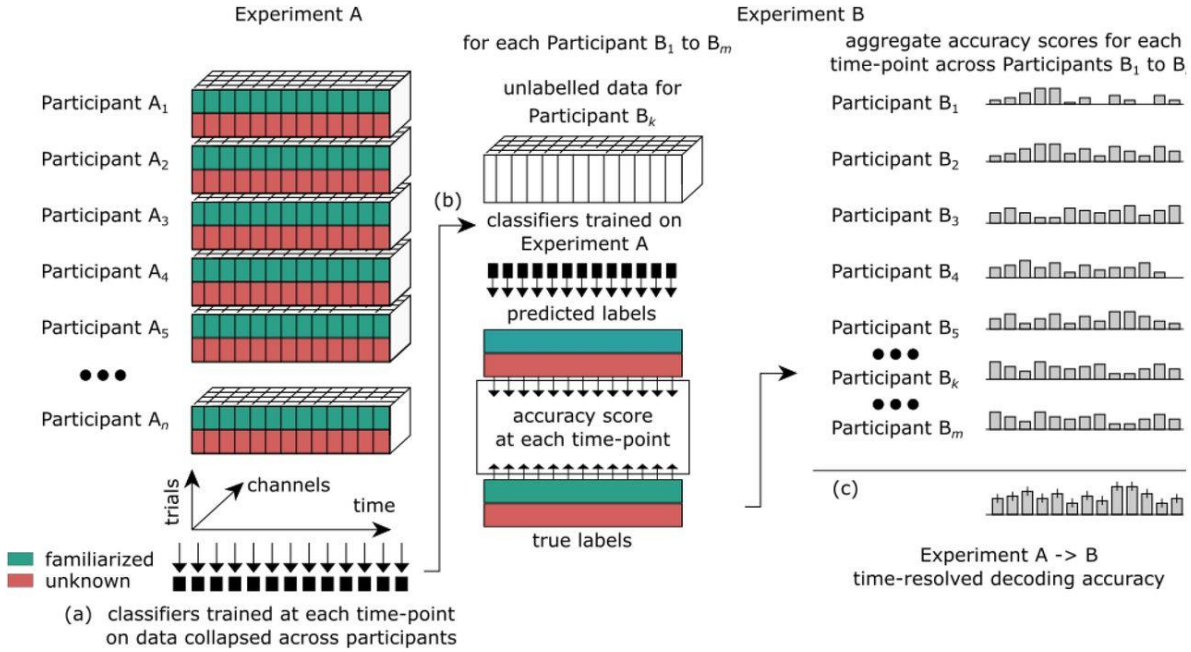

Figure 1. Cross-experiment decoding. (a) Trial × channel × time resolution EEG data from all participants in Experiment A is concatenated. At each time point, a classifier is trained to differentiate between familiarized and unknown trials. (b) These classifiers are then used to categorize the ERPs, at each corresponding time-point in Experiment B, for each participant separately. (c) The subject-level accuracy scores are aggregated to yield the time-resolved decoding accuracy for Experiments A → B.

EEG was recorded using a 64-channel Biosemi Active II system (512 Hz sampling rate; bandwidth: DC 461 to 120 Hz) in a dimly lit, electrically shielded, and sound–attenuated chamber. Data were bandpass filtered between 0.1 and 40 Hz, segmented between −200 and 1300 ms and baseline corrected to the 200 ms preceding the stimulus presentation. The data were downsampled to 100 Hz resolution, and no artifact rejection was performed (Grootswagers et al. 2017). Processing was carried out using MNE-Python (Gramfort et al. 2013).

Below is a short overview of the three experiments described in the report:

Perceptual Familiarization

Forty-two participants. Stimuli: 4 previously unknown female identities with 10 ambient images each. Forty repetitions of each image. Familiarization: sorting task for two of the 4 identities immediately prior to the EEG recording. The two to-be-familiarized identities were randomly chosen from the 6 possible permutations of the 4 IDs for each participant. Task: detection of slightly rotated images.

Media Familiarization

Twenty-four participants. Stimuli: 4 previously unknown (two male and two female) identities with 2 × 20 ambient images each, one image repeated 13 times. Familiarization: Watching a TV series with one male and one female person in lead roles between the pre- and post-familiarization EEG recordings. The to-be-familiarized identities were based on the series and were assigned randomly to the participants. Task: detection of repeated images.

Personal Familiarization

Twenty-three participants. Stimuli: 4 previously unknown female identities, with 10 ambient images each, one image repeated 22 times in a session. Familiarization: ca. one-hour personal interaction with two of the four identities on 3 consecutive days between pre- and post-familiarization EEG recordings. The to-be-familiarized identities were the same for all participants. Task: detection of rotated images.

Analysis

We used data from the post-familiarization phases of these experiments, using a cross-participant, cross-experiment decoding approach (Figure 1). Each iteration of the analysis used data from two out of the three experiments. The data was standardized within participants and across electrodes. The epoched EEG from all trials and all channels was concatenated from all participants in one experiment. At each of the 150 time points (−200 to 1300 ms relative to stimulus presentation onset, sampled at 100 Hz), linear discriminant analysis classifiers (LDA) were trained to categorize familiarized and unknown identities. These classifiers were then used to assess prediction accuracy for familiarity in the other experiment, for each participant separately.

To investigate the temporal organization of information processing stages, we used temporal generalization analysis. For this, the classifiers were trained on all timepoints in one experiment and tested on the data at every timepoint in the other, organized in a cross-temporal (training times × testing times) decoding accuracy matrix. We reasoned that if a classifier can generalize from one timepoint to another across experiments, similar information processing may be indicated at those time points. Furthermore, the temporal generalization method can reveal the stable, or dynamically evolving nature of the neural code that underlies above-chance decoding. For example, significant decoding accuracies clustered along the diagonal may suggest chained or isolated sets of generators, while a square-shaped generalization matrix indicates a stable neural code (King and Dehaene 2014).

To achieve a finer spatial resolution, we repeated the procedure using a region of interest (ROI) and a searchlight approach. In the ROI analysis, similarly to (Ambrus, Kaiser, et al. 2019) and Ambrus et al. (2021), we pre-defined six scalp locations along the medial (left and right) and coronal (anterior, center, and posterior) planes (see Supplementary Figure 1), and used these subsets of channels for training and testing. In the searchlight analysis, all channels were systematically tested by creating quasi-ROIs that also included the neighboring electrodes and conducted the same time-resolved analysis steps as described above (see Supplementary Figure 2).

Statistical Testing

In order to increase signal-to-noise ratio, a moving average of 30 ms (3 consecutive time-points) was used on all cross experiment decoding accuracy data at the participant level (Kaiser et al. 2016; Ambrus, Kaiser, et al. 2019). For the ROI-based analyses, to test if classifiers on a given experiment can decode the data in another experiment, the decoding accuracies were entered into two-tailed,

one-sample cluster permutation tests (10 000 iterations) against chance (50%). We also tested cross experiment decoding accuracies across 6 train/test pairings

with two-tailed cluster permutation tests with 10 000 iterations. For the searchlight analysis, two-tailed spatio-temporal cluster permutation tests were used against chance level (50%), with 10 000 iterations.

Additional exploratory analyses were carried out to probe the reliability of decoding on participant-level using a bootstrapping method (Di Nocera and Ferlazzo 2000; Wiese et al. 2019). In this analysis, predicted labels were randomly reassigned (10 000 iterations) to the trial conditions, and at each reassignment, an accuracy score was calculated. Reliable effects were assumed if a participant's true accuracy score exceeded 95% of the values, calculated from the random resamplings. Sample-level 95% confidence intervals were calculated the following way: First, true/false labels (assuming independent, equal outcomes) were randomly assigned to each participant in the sample, and a sample-wide accuracy score was calculated. This procedure was repeated 50 000 times. We determined the cut-off by ascertaining the number of participants needed to score true to reach or exceed the 95% of the accuracy cores in the bootstrapped sample (n ≥ 95%CI = Perceptual: 26 [61.9%], Media: 16 [66.6%], Personal: 15 [65.2%]).

The statistical analyses were conducted using python, MNE Python (Gramfort et al. 2013), scikit-learn (Pedregosa et al. 2011), and SciPy (Virtanen et al. 2020).

Results

All Electrodes

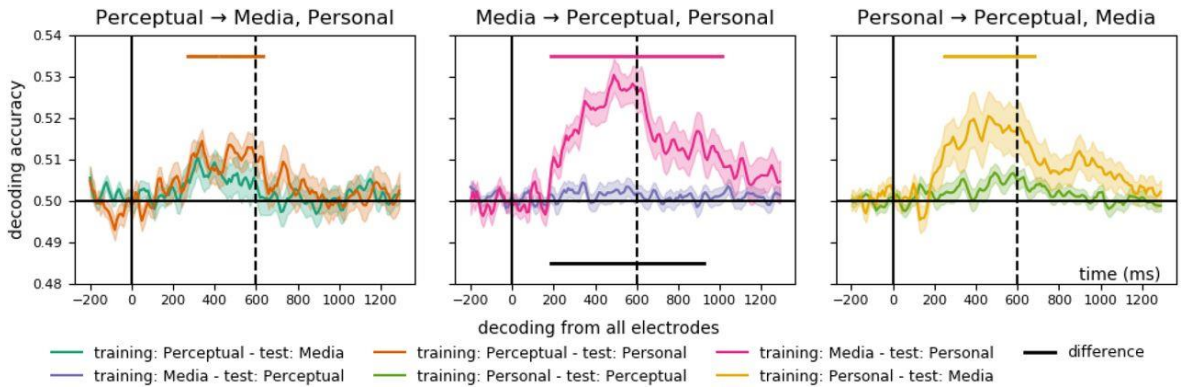

Figure 2. Time-resolved cross-experiment decoding accuracies on all electrodes. Horizontal markers denote clusters with significantly different decoding accuracies against chance (top markers) and between-pair differences (bottom markers; two-tailed cluster permutation tests, $p < 0.05$). Shaded ranges denote standard errors. Note that this analysis is the equivalent of taking the diagonal in the temporal generalization analysis (Figure 4.). For detailed statistics on the regions of interest see Supplementary Figure 1 and Supplementary Table 1.

Out of the six train-test cross-experiment decoding analyses on the all-electrodes data, significant familiarity decoding effects were observed in three, involving all three experiments, overlap ping between 270 and 630 ms (Figure 2., black significance markers) and peaking between 330 and 500 ms. Decodability of familiarity was mutual between the Media and the Personal familiarization experiments (Media ↔ Personal), with a significant cluster between 250 and 680 ms, peaking at

380 ms (peak t_{24} = 2.86, peak Cohen's d = 0.57) in Personal → Media, and a cluster between 190 and 1010 ms, peaking at 500 ms (peak t_{22} = 7.24, peak Cohen's d = 1.51) in Media → Personal direction. Furthermore, in Perceptual → Personal analysis a cluster between 270 and 410 ms with a peak at 330 ms (peak t_{22} = 4.36, Cohen's d = 0.91), and between 430 and 630 ms (peak t_{22} = 4.11, peak Cohen's d = 0.86) was observed. Although no significant cross-experiment decoding effect was seen between the Media and Perceptual familiarization experiments, for completeness, statistics on these non-significant pairs will be reported as well in the following sections.

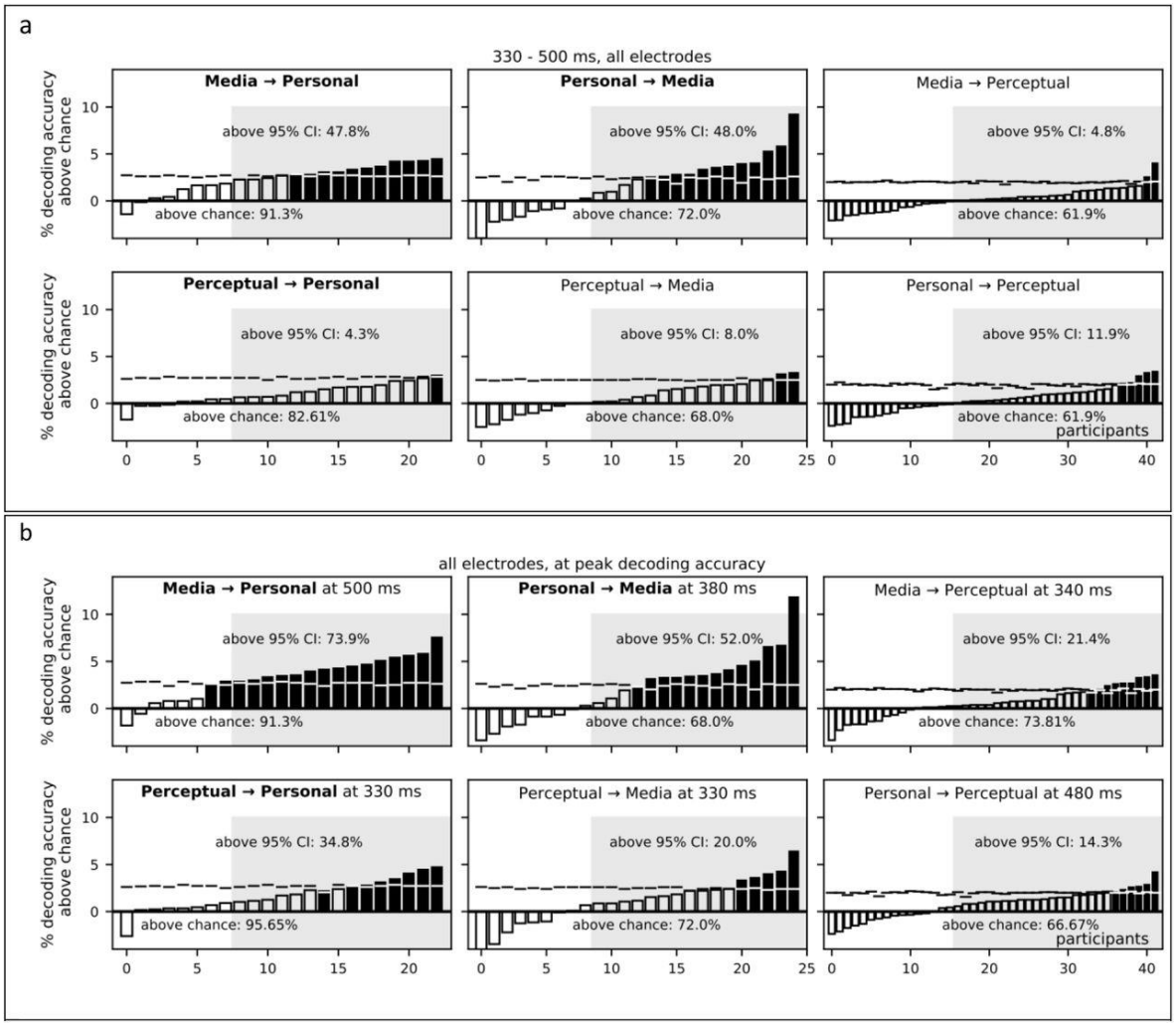

Figure 3. Cross-experiment familiarity decoding at a single participant-level, using bootstrapping analysis on decoding data from all electrodes. Each participant's decoding accuracy is presented separately, with filled bars indicating values exceeding the bootstrapped 95% confidence interval (horizontal markers). (a) Results of the overlapping 330–500 ms time windows (b) results at their respective peaks. Gray shaded areas denote the bootstrapped sample level 95% confidence intervals.

A bootstrapping analysis between the overlapping peak decoding time intervals (320–500 ms) revealed that the majority of the participants' accuracy scores lay above chance level, with 8% (Perceptual → Media), 4.3% (Perceptual → Personal) 47.8% (Media → Personal), and 48% (Personal → Media) of participants' scores reaching the 95% confidence interval (Figure 3a). To establish an upper bound on subject-level reliability, we repeated the bootstrapping analysis separately for all train/test pairs at their respective peaks. Again, the majority of scores exceeded the chance level in all cases, with 21.4% (Media → Perceptual), 14.3% (Personal → Perceptual), 20%

(Perceptual → Media), 34.8% (Perceptual → Personal) 74% (Media → Personal), and 52% (Personal → Media) of participants' scores over the 95% confidence interval (Figure 3b).

The temporal generalization analysis (Figure 4, Supplementary Figure 2.) revealed a sustained above-chance decoding accuracy starting around 170 ms, lasting consistently to around 600 ms or in some cases, beyond. Media predicted, between 180 ms to the end of the epoch from Personal between 80 ms onwards (cluster p = 0.0002). Reversely, Personal predicted, from 160 ms, Media, from 190 to 700 ms (cluster p = 0.017). Finally, Perceptual, between 170 and 1170 ms, predicted Personal, from 80 to 1010 ms, (cluster p = 0.019).

Regions of Interest

To track representational organization across electrode space, we repeated the above analysis across the 6 electrode clusters also used in previous studies (Ambrus et al. 2019, 2021)). For further details see Supplementary Figure 1 and Supplementary Table 1.

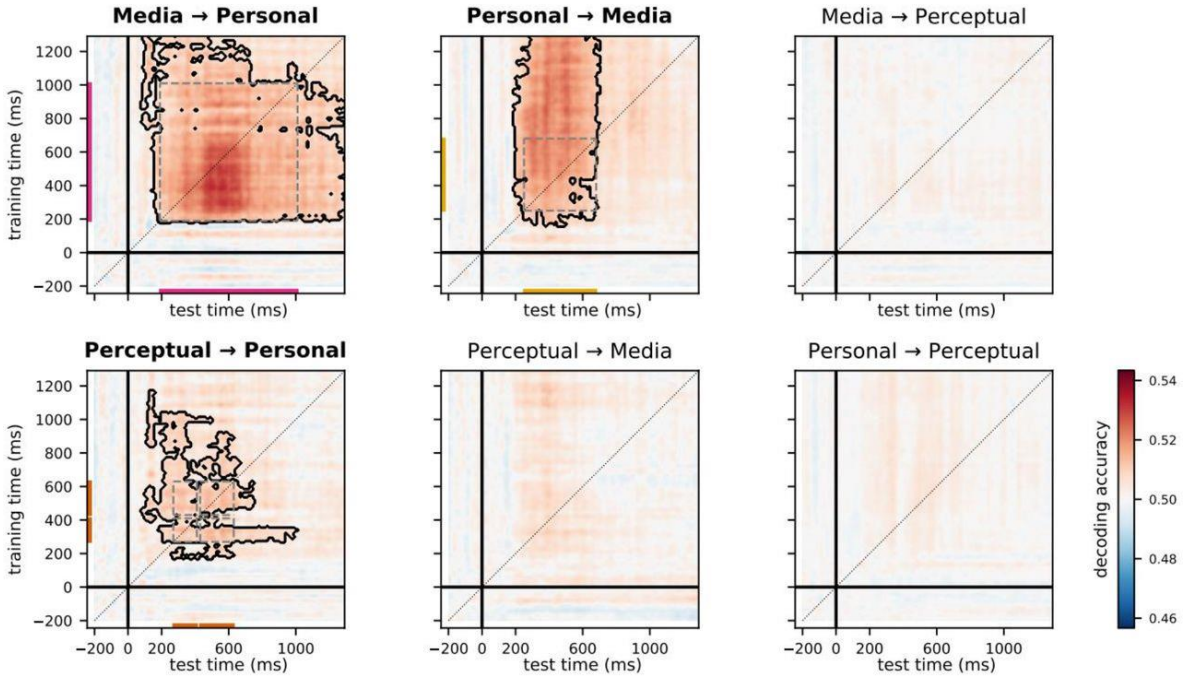

Figure 4. Cross-experiment temporal generalization analysis on all electrodes. For the results of the temporal generalization analyses separately in the different ROIs, see Supplementary Figure 2.

ROI analyses shown familiarity effects at posterior and central areas, mainly falling within the 300–600 ms interval. In Personal → Media, a right posterior cluster with an extent of 250–670 ms, peaking at 490 ms (peak t_{24} = 4.3, peak Cohen's d = 0.86) two left posterior clusters at 180–340 ms with a peak at 270 ms (peak t_{24} = 2.83, peak Cohen's d = 0.57) and 360–800 ms with a peak at 520 ms (peak t_{24} = 4.57, peak Cohen's d = 0.91), a right central cluster between 340 and 1010 ms with a peak at 530 ms (peak t_{24} = 3.98, peak Cohen's d = 0.80), and a left central cluster between 380 and 640 ms with a peak at 500 ms (peak t_{24} = 2.44, peak Cohen's d = 0.59) emerged. In Media → Personal, a right posterior cluster between 200 and 1290 ms with a peak at 470 ms (peak t_{22} = 7.86, peak Cohen's d = 1.64), three left posterior clusters, between 190 and 290 ms with a peak at 270 ms (peak t_{22} = 3.90, peak Cohen's d = 0.82), between 320 and 990 ms with a peak at 480 ms (peak t_{22} = 4.96, peak Cohen's d = 1.03), and a late 1010–1170 ms cluster with a peak at 1110 ms (peak t_{22} = 3.58, peak Cohen's d = 0.75) and a right central cluster between 230 and 680 ms with a peak at 350 ms (peak t_{22} = 4.50, peak Cohen's d = 1.04) were shown. In Perceptual → Personal, a right posterior cluster

between 220 and 630 ms with a peak at 490 ms (peak t_{22} = 6.1, Cohen's d = 1.27), a left posterior cluster between 480 and 640 ms with a peak at 520 ms (peak t_{22} = 5.29, Cohen's d = 1.10), two right central clusters between 260 and 370 ms with a peak at 330 ms (peak t_{22} = 5.27, Cohen's d = 1.10) and between 450 and 630 ms with a peak at 540 ms (peak t_{22} = 5.17, Cohen's d = 1.08), two left central clusters between 260 and 360 ms with a peak at 330 ms (peak t_{22} = 3.58, Cohen's d = 0.75) and 480 to 580 ms with a peak at 500 ms (peak t_{22} = 3.47, Cohen's d = 0.72) emerged. In Personal → Perceptual, two posterior clusters, one on the right between 480 and 580 ms with a peak at 560 ms (peak t_{41} = 3.31, peak Cohen's d = 0.51) and one on the left between 470 and 590 ms peaking at 520 ms (peak t_{41} = 3.12, peak Cohen's d = 0.48) were found. In Perceptual → Media, a single right central cluster between 260 and 560 ms with a peak at 320 ms (peak t_{24} = 3.59, peak Cohen's d = 0.72) was observed. In Media → Perceptual, no significant effect was found.

Searchlight

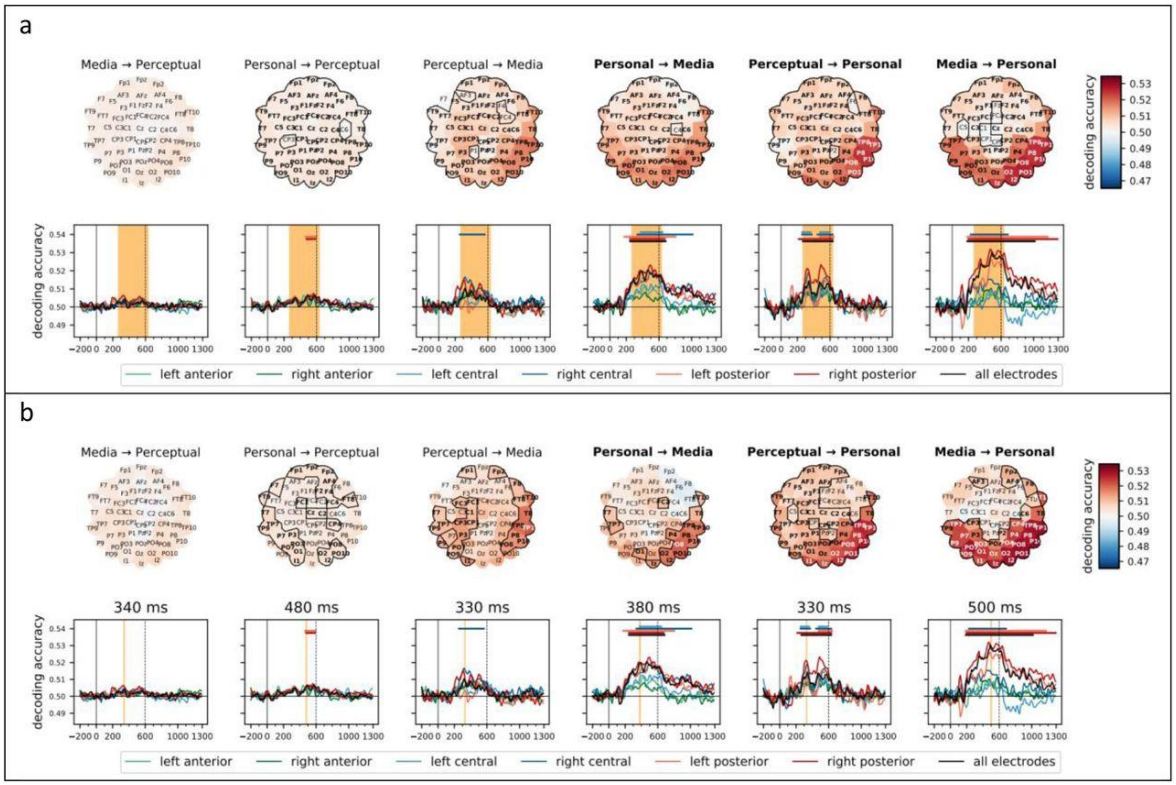

Figure 5. Region-of-interest and searchlight analyses. In three out of six train/test pairs involving all three experiments, significant decoding accuracies based on all electrodes (black horizontal marker) overlapped between 270 and 630 ms after stimulus onset (a). Further two train/test pairs revealed significant clusters at posterior or central ROIs within this interval. Peak decoding accuracies in all analyses (b) fell between this overlapping interval. The top panel scalp maps show the averaged searchlight-based decoding accuracies (electrodes belonging to significant spatio-temporal clusters marked) in the different train/test evaluations averaged over the overlapping timepoints. The bottom part shows the time-resolved ROI-based decoding results. Horizontal markers denote clusters with significantly different decoding accuracies against chance (two-tailed cluster permutation test, p < 0.05). For detailed results, see Supplementary Figure 3.

Apart from Media → Perceptual, extensive significant spatio-temporal clusters, encoding familiarity, were observed in several searchlight analyses. In Media → Personal a significant cluster (cluster p < 0.001), starting from 180 ms at bilateral temporo-parieto-occipital electrodes, was observed. Also starting at 180 ms (electrode I1), there was a significant cluster found in Personal → Media

(cluster p = 0.014), lasting until 700 ms after stimulus onset. A significant cluster with an even earlier onset (100 ms, at Oz and POz) was observed in Perceptual → Personal (cluster p < 0.001), lasting until 1210 ms. Between 210 and 680 ms, Perceptual → Media (cluster p = 0.01, starting at PO8 and P4) and between 410 and 870 ms, Personal → Perceptual (starting at FT9, cluster p = 0.007) also yielded significant clusters (Figure 5).

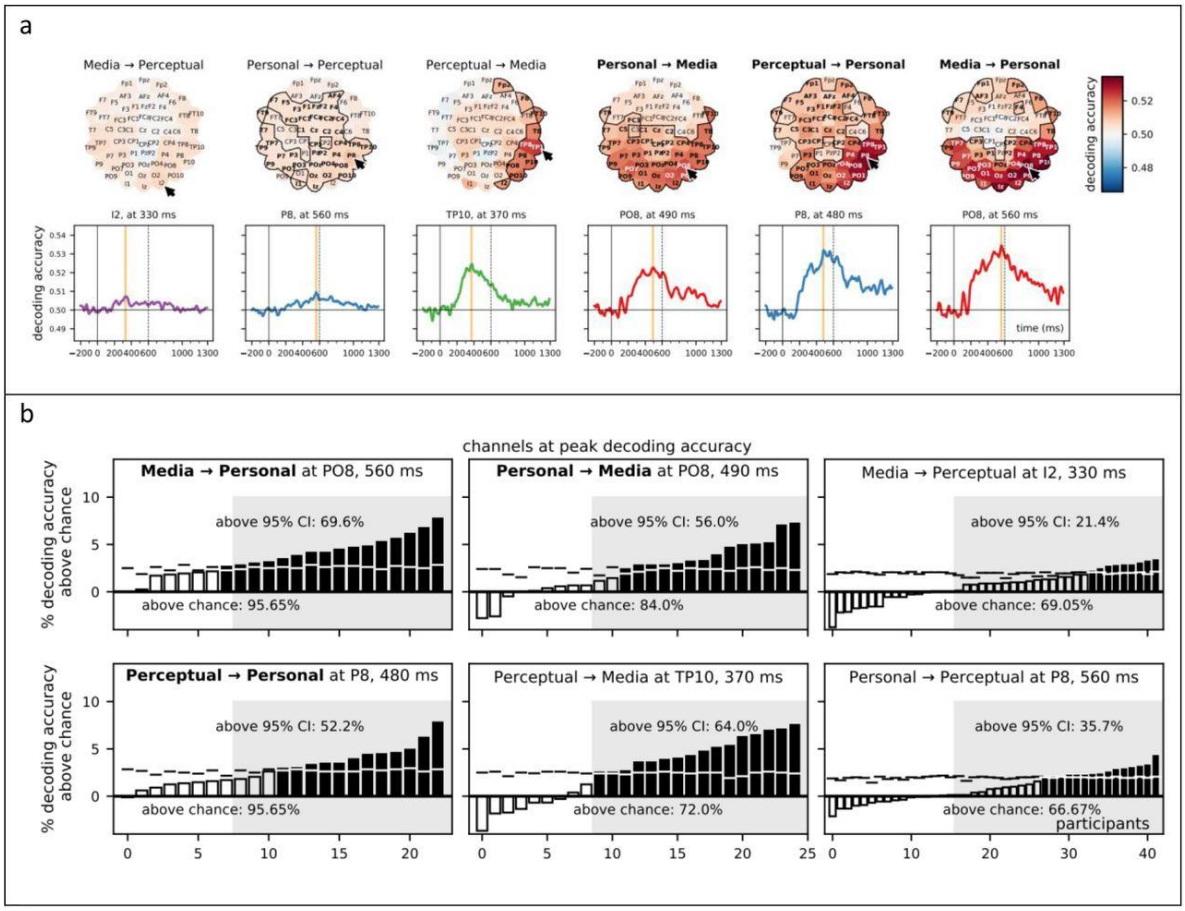

Figure 6. Cross-experiment searchlight analysis. Electrodes with the highest peak decoding accuracy at their respective peak latencies. (a) Highest peak decoding accuracies are seen over the right-hemisphere occipito-temporo-parietal electrodes (black arrows), ranging from 330 to 560 ms. (b) Bootstrapping analyses on the data of these electrodes at peak accuracy times revealed above-chance decoding in the majority of the participants in every cross-experiment combination. The decoding accuracy of individual participants is shown, with filled bars indicating values exceeding the bootstrapped 95% confidence interval (horizontal markers). Gray shaded areas denote the bootstrapped sample level 95% confidence intervals. Pairs with significant clusters in decoding from all electrodes are highlighted in bold typeface.

Analysis of the searchlight results revealed peak decoding accuracies at right parieto-occipito-temporal sites in all evaluations. In both Media → Personal and Personal → Media, maximum decoding accuracy was found at PO8, peaking at 560 ms (peak Cohen's d = 1.83) and 490 ms (peak Cohen's d = 0.89), respectively. In Perceptual → Personal the peak decoding accuracy was at P8, with a peak at 480 ms (peak Cohen's d = 1.55). In Perceptual → Media, peak decoding accuracy was observed at TP10 at 370 ms (peak Cohen's d = 0.85). In Personal → Perceptual, peak decoding accuracy was found at P8 at 560 ms (peak Cohen's d = 0.61), and in Media → Perceptual at I2 at 330 ms (peak Cohen's d = 0.32). Figure 6 shows the scalp distributions in the six cross-experiment searchlight decoding evaluations at and the bootstrap-based subject-level reliability calculations at their respective peak decoding latencies. For further details see Supplementary Figure 3.

Additional Analyses

We also compared the results of the cross-experiment analyses to within-experiment, leave-one-participant-out results. These comparisons show no significant difference between Personal → Media and within-Media, but a prominent early within Personal signal (peaking at 130 ms) was missing in both the Perceptual → Personal, and Media → Personal cross experiment analyses. This is accounted for by the fact that early ERP signals are sensitive to low-level image statistics, and in the Personal experiment these were diagnostic as the familiarized and unknown stimuli were the same for

all participants (Supplementary Information 1). The post 200 ms cross-experiment classifiers in the Media and Personal experiments did not underperform those that were trained within-experiment, and the general shape of the familiarity effects are remarkably similar in both cases, despite the differences in stimulus identities, stimulus gender, mode of familiarization, and experimental task.

We conducted several additional analyses to rule out various sources of bias in our cross-experimental decoding method. The procedures and results of these are presented in the Supplementary Information 2–4. It is important to account for the possibility that besides familiarity, neural responses to other properties of the stimuli aid the classification. To rule out the effects of such features (e.g., low-level image statistics), we repeated the time-resolved cross-experiment decoding procedure, iteratively training on the Post-familiarization phase, and testing on the pre-familiarization phase of the experiments, where the stimuli were the same, but not yet familiar to the participants. We found no significant clusters in any of the analyses, suggesting that non-familiarity-related stimulus properties can be ruled out as confounds (Supplementary Information 2). To rule out that the effects observed in the Perceptual → Personal and Perceptual → Media analyses were affected by the relatively larger number of participants in the Perceptual experiment, we performed 100 iterations of the analyses where the Perceptual experiment served as the training set, with 24 randomly chosen participants at each iteration (Supplementary Information 3). Finally, to rule out the possibility that highly discriminable features come from only a few participants, we conducted cross experiment, cross-participant decoding analyses, i.e., iteratively training and testing on each participant across the experiments (see Supplementary Information 4). These analyses yielded similar results to our original, cross-experiment analyses, albeit with considerably lower mean decoding accuracies (due to the more limited data per classification). We found no indication of a few high signal-to-noise data points biasing the results.

Discussion

The current analysis is based on data from Ambrus et al. 2021 which explored the temporal dynamics of emerging face identity and familiarity information under different of familiarization conditions. Time-resolved representational similarity analysis of EEG data revealed that the level of familiarization has a robust effect on familiarity representations: they are strongly visible over posterior and central regions following personal, somewhat weaker after media familiarization, and they are absent following perceptual familiarization.

In this present study, we set out to uncover the existence of shared face familiarity signal, across participants, familiarization contexts, and stimulus identities. We applied a cross-experiment decoding approach where evoked responses from participants in one experiment are decoded using classifiers trained on the aggregated data of the participants of another study. It is important to note that three experiments of the current study differed in 1) the mode and length of familiarization, 2) the stimulus material, 3) the number of images of a given identity, 4) the task, and 5) the participants tested. It is

also worth taking note of the commonalities between the experiments, such as the Perceptual and Personal utilizing the same attention task (rotation detection), while in Media, a 1-back task was used. As Huang et al. (2017) have shown, task dependency might have an influence on the decodability of the familiarity signal. Furthermore, while for the perceptual and media familiarization an all-female stimulus set was used, in the case of the media familiarization both male and female stimuli were presented.

Despite all these substantial differences between the three experiments, we found significant sustained cross-experiment familiarity decoding accuracies, most prominently in the Media ↔ Personal, and the Perceptual → Personal familiarization conditions, overlapping between 270–630 ms. Bootstrapping analyses within the peak accuracy intervals (330–500 ms) have shown above-chance decoding in most of the participants, albeit the participant-level reliability did not reach the sample-level 95% confidence interval (Figure 3a). Additional ROI-and searchlight-based analyses revealed bilateral posterior and central effects, with a more pronounced right-hemisphere weight.

We observed the most evident cross-experiment familiarity effect between the Media and Personal familiarization experiments, where the depth of familiarization was arguably the highest. In the Media experiment, in the span of two weeks, participants viewed a season of a television series, while in the Personal experiment, participants interacted with the experimentally familiarized identities personally for ca. 1 hour on 3 consecutive days. Somewhat unexpectedly, a similar effect emerged in Perceptual → Personal albeit more restricted in time. This is surprising as no significant familiarity effect was observed in the Perceptual experiment, in which identities were familiarized through a very short sequential sorting task (based on Andrews et al. 2015), as implemented in Ambrus, Dotzer, et al. (2017)). Although no further significant decoding effects on all electrodes were found, in Perceptual → Media a right-central cluster with an onset and duration similar to other train/test pairs was observed, while in Personal → Perceptual a small bilateral posterior effect was seen, also falling within the overlapping time windows of the strongest effects found in other decoding pairs. Finally, no familiarity-related cross-experiment decoding effects were observed in Media → Perceptual.

There was some variation in the onset and duration of the effects, with searchlight and temporal generalization analyses flagging time points as early as ca. 100 and 160 ms, and ROI analyses showing onsets at around 180–200 ms in some cases. Literature regarding early effects is somewhat inconsistent (Ramon and Gobbini 2018)—while some reported no familiarity-related modulation in such early phases (Huang et al. 2017), ERP amplitude increase (Kloth et al. 2006), and decrease (Todd et al. 2008) have also been described.

Recently, In an MEG-MVPA experiment Dobs et al. (2019) found a familiarity-related component about 400–600 ms after stimulus onset, using familiar and unfamiliar celebrities as stimuli. The authors hypothesized that this identity-independent familiarity effect may reflect memory-related activations or affective responses. Wiese et al. (2019) also described an ERP component elicited by highly familiar versus unfamiliar faces. This sustained familiarity effect (SFE) started at around 200 ms after stimulus onset and reached its maximum between 400 and 600 ms as well. The source of this effect is theorized to lie within the ventral visual pathway, and its magnitude was found to be modulated by the level of familiarity (larger for contrasts with personally familiar faces compared to lecturers or celebrities). This led the authors to suggest that the SFE may be driven by the integration of perceptual and affective information. Finally, Karimi-Rouzbahani et al. (2021) also observed a familiarity-related effect starting around 200 ms and peaking after ca. 400, with the highest ERP amplitude elicited by the participants own face, followed by personally familiar, celebrity, and unfamiliar faces. The most stable cross-experiment effects were also observed in the 400–600 ms time-window, with peak decoding accuracies between 330–500 ms, supporting these above-mentioned results. While interindividual

differences, regarding the recognition of faces play a crucial role, these studies also propose the idea of a shared, fundamental neural representation of face familiarity: Based on their temporal and spatial characteristics, we suggest that the familiarity effects, reported by the previous studies and the cross-experiment decoding of the current study are related, and are indicative of a robust and general familiarity effect, which is largely independent of participants, experimental stimuli, and the method of familiarization.

Where significant familiarity-related effects were present, temporal generalization analyses on all electrodes revealed a sustained above-chance decoding performance starting around 200 ms, lasting consistently to around 600 ms or in some cases, beyond. This suggests that the classifiers picked up on features generated by a single process, maintained over time (King and Dehaene 2014).

At this point, we can only speculate as to the nature of processing underlying this observed effect. Although it is difficult to make inferences regarding the anatomical structures generating these signals, its occipito-temporal dominance is consistent with sources reported in relation to the ventral visual pathway, and parts of the core and extended face networks are most certainly involved (Gobbini and Haxby 2007; Kovács 2020). The occipital face area (OFA), an early face-selective region that has been shown to take part in image-dependent lower-level feature analysis (Pitcher et al. 2007) is already differentially responsive to familiar and unfamiliar identities (Jonas et al. 2014; Ambrus, Dotzer, et al. 2017; Amado et al. 2018; Ambrus, Amado, et al. 2019), and may also play a causal role in the learning of new faces (Ambrus, Windel, et al. 2017). The fusiform face area (FFA) shows image-independent processing of face-information, it is therefore highly probable that its normal functioning is central to the recognition of familiar identities (Kanwisher et al. 1997). Finally, the superior temporal sulcus (STS) is more sensitive to dynamic/changeable visual features such as facial expressions (Zhang et al. 2016; Direito et al. 2019) (but see also (Calder and Young 2016)) that may also carry diagnostic, identity-specific information, thus boosting familiarity signals. Also worth noting here that face-responsive cells in the monkey superior temporal polysensory area codes for familiarity and social status (Young and Yamane 1992), and that classifiers trained on fMRI signals for face identities in the right posterior STS can also differentiate between voices, and vice versa (Tsantani et al. 2019).

The relatively late peak decoding latency we observed may be an indication that it depends, at least partially, on post-perceptual processing that is fed back from more modality-independent, memory-related cortical areas. For example, regions considered to be outside the core face networks, such as different extrastriate visual areas, the structures in the anterior and medial temporal lobe (MTL) have been reliably demonstrated to exhibit stronger responses to familiar stimuli, including faces. The anterior temporal lobe (ATL), considered to be a semantic hub (Anzellotti 2017), is involved in associations of person-related semantics (Morton et al. 2021), e.g., a connection between a name and a face (Tsukiura et al. 2010). Structures within the MTL (e.g., the amygdala, perirhinal cortex and hippocampus) are involved in the storing and processing of biographical/autobiographical information related to faces, including the feelings of familiarity, and respond abruptly when sufficient information for familiar face recognition is accumulated (Ramon et al. 2015).

Some of our analyses yielded decoding direction asymmetries, i.e., the cross-classification performance between two given experiments depended on the decoding direction. This is most evident in the case of Perceptual ↔ Personal, where generalization failed in the Personal → Perceptual, but succeeded in the Perceptual → Personal direction.

In a recent study, van den Hurk and Op de Beeck 2019 elegantly demonstrated that such decoding direction asymmetries can be explained by the differences in signal-to-noise ratio (SNR) between the two datasets, with better generalization performance from the lower SNR to the higher SNR dataset. A lower SNR is indeed expected in the Perceptual experiment, with a brief, image-based sorting task, lasting a few minutes, compared to the other two experiments that involved more extensive familiarization. This SNR imbalance allows familiarity information to be extracted by the classifier from the Perceptual experiment data at training, but the higher noise in the signal prevents successful generalization in decoding. Thus, as van den Hurk and Op de Beeck (2019) suggest, the interpretation regarding significant generalization should be based on the superior performance direction. As such, the decoding direction asymmetry, and the lack of statistically significant familiarity effects in the Perceptual experiment (Ambrus et al. 2021; Supplementary Information 1) do not invalidate the cross-experiment decoding results, but instead demonstrate that the seeds of the familiarity effect are already present in purely image-based individuation. This seems to imply that contributions from semantic, autobiographical, and affective processes are less essential, as these facets played little role in the Perceptual familiarization experiment, thus memory processes related to face-feature-based recall might be more promising candidates. Still, it is possible that even short-term perceptual familiarization engages the whole cascade, for example because it is enough to trigger search processes in long term storage and/or semantic and affective hubs. Further research is needed to precisely pin down the exact cognitive machinery behind our results. For example, methods such as M/EEG-fMRI fusion (Cichy and Oliva 2020; Muukkonen et al. 2020), combining the spatial and temporal resolution of these techniques, may give us further insight.

On a methodological note, this study has shown that cross-experiment decoding is uniquely suited for finding general neural patterns that are indicative of a shared processing of information. It has the potential to be more sensitive than within-subject decoding, as it benefits from more training data and is less confounded by idiosyncratic participant-level effects and stimulus properties. We hope to see this method being utilized to advance our understanding of brain dynamics in the future.

Author statement

AD, GK, GGA contributed to the design and implementation of the research, to the analysis of the results and to the writing of the manuscript. GK was involved in providing funding sources for the study. All authors provided critical feedback and helped shape the study.

Notes

Conflict of Interest: No competing interests are declared.

Funding

The Deutsche Forschungsgemeinschaft (KO3918/5–1). Alexia Dalski is supported by a scholarship from the Honors Programme for Future Researchers at the Friedrich Schiller University Jena.

References

Amado C, Kovács P, Mayer R, Ambrus GG, Trapp S, Kovács G. 2018. Neuroimaging results suggest the role of prediction in cross-domain priming. Sci Rep. 8:10356.

Ambrus GG, Amado C, Krohn L, Kovács G. 2019. TMS of the occipital face area modulates cross-domain identity priming. Brain Struct Funct. 224:149–157.

Ambrus GG, Dotzer M, Schweinberger SR, Kovács G. 2017. The occipital face area is causally involved in the formation of identityspecific face representations. Brain Struct Funct.

Ambrus GG, Kaiser D, Cichy RM, Kovács G. 2019. The Neural Dynamics of Familiar Face Recognition. Cereb Cortex. 29:4775–4784.

Ambrus GG, Windel F, Burton AM, Kovács G. 2017. Causal evidence of the involvement of the right occipital face area in face-identity acquisition. Neuroimage. 148:212–218.

Andrews S, Jenkins R, Cursiter H, Burton AM, Andrews S, Jenkins R, Cursiter H, Telling AMB, Andrews S, Jenkins R, Cursiter H, Burton AM. 2015. Telling faces together: Learning new faces through exposure to multiple instances. Q J Exp Psychol. 0218:2041–2050.

Anzellotti S. 2017. Anterior temporal lobe and the representation of knowledge about people. Proc Natl Acad Sci U S A.

Barragan-Jason G, Cauchoix M, Barbeau EJ. 2015. The neural speed of familiar face recognition. Neuropsychologia. 75:390–401.

Buttle H, Raymond JE. 2003. High familiarity enhances visual change detection for face stimuli. Percept Psychophys. 65:1296–1306.

Caharel S, d'Arripe O, Ramon M, Jacques C, Rossion B. 2009. Early adaptation to repeated unfamiliar faces across viewpoint changes in the right hemisphere: Evidence from the N170 ERP component. Neuropsychologia. 47:639–643.

Caharel S, Poiroux S, Bernard C, Thibaut F, Lalonde R, Rebai M. 2002. ERPs associated with familiarity and degree of familiarity during face recognition. Int J Neurosci. 112:1499–1512.

Caharel S, Ramon M, Rossion B. 2013. Face Familiarity Decisions Take 200 msec in the Human Brain: Electrophysiological Evidence from a Go / No-go Speeded Task. 81–95.

Calder AJ, Young AW. 2016. Understanding the recognition of facial identity and facial expression. Facial Expr Recognit Sel Work Andy Young. 6:41–64.

Cichy RM, Oliva A. 2020. A M/EEG-fMRI Fusion Primer: Resolving Human Brain Responses in Space and Time. Neuron.

Debruille JB, Guillem F, Renault B. 1998. ERPs and chronometry of face recognition: Following-up Seeck et al. and George et al. Neuroreport. 9:3349–3353.

Di Nocera F, Ferlazzo F. 2000. Resampling approach to statistical inference: Bootstrapping from event-related potentials data. Behav Res Methods, Instruments, Comput. 32:111–119.

Direito B, Lima J, Simões M, Sayal A, Sousa T, Lührs M, Ferreira C, Castelo-Branco M. 2019. Targeting dynamic facial processing mechanisms in superior temporal sulcus using a novel fMRI neurofeedback target. Neuroscience. 406:97–108.

Dobs K, Isik L, Pantazis D, Kanwisher N. 2019. How face perception unfolds over time. Nat Commun. 10.

Duchaine B, Yovel G. 2015. A Revised Neural Framework for Face Processing. Annu Rev Vis Sci. 1:393–416.

Ellis HD, Lewis MB. 2001. Capgras delusion: A window on face recognition. Trends Cogn Sci.

Gobbini MI, Haxby J V. 2007. Neural systems for recognition of familiar faces. Neuropsychologia. 45:32–41.

Gramfort A, Luessi M, Larson E, Engemann DA, Strohmeier D, Brodbeck C, Goj R, Jas M, Brooks T, Parkkonen L, Hämäläinen M. 2013. MEG and EEG data analysis with MNE-Python. Front Neurosci.

Grootswagers T, Wardle SG, Carlson TA. 2017. Decoding dynamic brain patterns from evoked responses: A tutorial on multivariate pattern analysis applied to time series neuroimaging data. J Cogn Neurosci. 29:677–697.

Huang W, Wu X, Hu L, Wang L, Ding Y, Qu Z. 2017. Revisiting the earliest electrophysiological correlate of familiar face recognition. Int J Psychophysiol. 120:42–53.

Johnston P, Overell A, Kaufman J, Robinson J, Young AW. 2016. Expectations about person identity modulate the face-sensitive N170. Cortex. 85:54–64.

Johnston RA, Edmonds AJ. 2009. Familiar and unfamiliar face recognition: A review. Memory. 17:577–596.

Jonas J, Rossion B, Krieg J, Koessler L, Colnat-Coulbois S, Vespignani H, Jacques C, Vignal JP, Brissart H, Maillard L. 2014. Intracerebral electrical stimulation of a face-selective area in the right inferior occipital cortex impairs individual face discrimination. Neuroimage. 99:487–497.

Kaiser D, Oosterhof NN, Peelen M V. 2016. The Neural Dynamics of Attentional Selection in Natural Scenes. J Neurosci. 36:10522–10528.

Kanwisher NG, McDermott J, Chun MM. 1997. The fusiform face area: a module in human extrastriate cortex specialized for face perception. J Neurosci. 17:4302–4311.

Kaplan JT, Man K, Greening SG. 2015. Multivariate cross-classification: Applying machine learning techniques to characterize abstraction in neural representations. Front Hum Neurosci. 9.

Karimi-Rouzbahani H, Remezani F, Woolgar A, Rich A, Ghodrati M. 2020. Perceptual difficulty modulates the direction of information flow in familiar face recognition. bioRxiv. 2020.08.10.245241.

King JR, Dehaene S. 2014. Characterizing the dynamics of mental representations: The temporal generalization method. Trends Cogn Sci.

Kloth N, Dobel C, Schweinberger SR, Zwitserlood P, Bölte J, Junghöfer M. 2006. Effects of personal familiarity on early neuromagnetic correlates of face perception. Eur J Neurosci. 24:3317–3321.

Kovács G. 2020. Getting to know someone: Familiarity, person recognition, and identification in the human brain. J Cogn Neurosci. 32:2205–2225.

Landi SM, Freiwald WA. 2017. Two areas for familiar face recognition in the primate brain. Science (80-). 357:591–595.

Millen AE, Hancock PJB. 2019. Eye see through you! Eye tracking unmasks concealed face recognition despite countermeasures. Cogn Res Princ Implic. 4.

Morton NW, Zippi EL, Noh S, Preston AR. 2021. Semantic knowledge of famous people and places is represented in hippocampus and distinct cortical networks. J Neurosci.

Muukkonen I, Ölander K, Numminen J, Salmela VR. 2020. Spatio-temporal dynamics of face perception. Neuroimage. 209.

Pedregosa F, Varoquaux G, Gramfort A, Michel V, Thirion B, Grisel O, Blondel M, Prettenhofer P, Weiss R, Dubourg V, others. 2011. Scikit-learn: Machine learning in Python. J Mach Learn Res. 12:2825–2830.

Persike M, Meinhardt-Injac B, Meinhardt G. 2013. The preview benefit for familiar and unfamiliar faces. Vision Res. 87:1–9.

Pitcher D, Walsh V, Yovel G, Duchaine B. 2007. TMS evidence for the involvement of the right occipital face area in early face processing. Curr Biol. 17:1568–1573.

Ramon M, Caharel S, Rossion B. 2011. The speed of recognition of personally familiar faces. Perception. 40:437–449.

Ramon M, Gobbini MI. 2018. Familiarity matters: A review on prioritized processing of personally familiar faces. Vis cogn. 26:179–195.

Ramon M, Sokhn N, Caldara R. 2019. Decisional space modulates visual categorization – Evidence from saccadic reaction times. Cognition. 186:42–49.

Ramon M, Vizioli L, Liu-Shuang J, Rossion B. 2015. Neural microgenesis of personally familiar face recognition. Proc Natl Acad Sci. 112:E4835--E4844.

Rosenzweig G, Bonneh YS. 2019. Familiarity revealed by involuntary eye movements on the fringe of awareness. Sci Rep. 9.

Sanchez JFQ, Liu X, Zhou C, Hildebrandt A. 2021. Nature and Nurture Shape Structural Connectivity in the Face Processing Brain Network. Neuroimage. 117736.

Todd RM, Lewis MD, Meusel LA, Zelazo PD. 2008. The time course of social-emotional processing in early childhood: ERP responses to facial affect and personal familiarity in a Go-Nogo task. Neuropsychologia. 46:595–613.

Tranel D, Damasio AR. 1985. Knowledge without awareness: An autonomic index of facial recognition by prosopagnosics. Science (80-). 228:1453–1454.

Tsantani M, Kriegeskorte N, McGettigan C, Garrido L. 2019. Faces and voices in the brain: A modality-general person-identity representation in superior temporal sulcus. Neuroimage. 201.

Tsukiura T, Mano Y, Sekiguchi A, Yomogida Y, Hoshi K, Kambara T, Takeuchi H, Sugiura M, Kawashima R. 2010. Dissociable roles of the anterior temporal regions in successful encoding of memory for person identity information. J Cogn Neurosci. 22:2226–2237.

van Belle G, Ramon M, Lefèvre P, Rossion B. 2010. Fixation patterns during recognition of personally familiar and unfamiliar faces. Front Psychol. 1:1–8.

van den Hurk J, Op de Beeck HP. 2019. Generalization asymmetry in multivariate cross-classification: When representation A generalizes better to representation B than B to A. bioRxiv.

Verhallen RJ, Bosten JM, Goodbourn PT, Lawrance-Owen AJ, Bargary G, Mollon JD. 2016. General and specific factors in the processing of faces. Vision Res.

Virtanen P, et al. 2020. SciPy 1.0: fundamental algorithms for scientific computing in Python. Nat Methods. 17:261–272.

Wiese H, Tüttenberg SC, Ingram BT, Chan CYX, Gurbuz Z, Burton AM, Young AW. 2019. A Robust Neural Index of High Face Familiarity. Psychol Sci. 30:261–272.

Wilmer JB, Germine L, Chabris CF, Chatterjee G, Williams M, Loken E, Nakayama K, Duchaine B. 2010. Human face recognition ability is specific and highly heritable. Proc Natl Acad Sci U S A. 107:5238–5241.

Yan X, Young AW, Andrews TJ. 2017. The automaticity of face perception is influenced by familiarity. Attention, Perception, Psychophys. 79:2202–2211.

Young MP, Yamane S. 1992. Sparse population coding of faces in the intertemporal cortex. Science (80-). 256:1327–1331.

Zhang H, Japee S, Nolan R, Chu C, Liu N, Ungerleider LG. 2016. Face-selective regions differ in their ability to classify facial expressions. Neuroimage. 130:77–90.